



# Transforming spent coffee grounds into a valuable resource for the enhancement of concrete strength

Rajeev Roychand<sup>\*,1</sup>, Shannon Kilmartin-Lynch<sup>2</sup>, Mohammad Saberian, Jie Li<sup>\*</sup>, Guomin Zhang, Chun Qing Li

School of Engineering, RMIT University, Melbourne, Victoria, Australia

## ARTICLE INFO

Handling Editor: Jian Zuo

### Keywords:

Spent coffee grounds  
Biochar  
Pyrolysis  
Concrete  
Strength development

## ABSTRACT

The decomposition of organic waste going to landfills produces methane gas, which is 21 times worse than CO<sub>2</sub> in its global warming potential. Spent coffee grounds (SCG) are one type of organic waste that makes up a significant proportion of the organic waste going to landfills. Therefore, it becomes imperative to look for a recycling solution to transform this waste into a valuable resource. The concrete industry has the potential to contribute significantly to increasing the recycling rate of this waste material. However, due to its high organic content, it is unsuitable to be used directly in structural concrete. Therefore, this experimental project looks at pyrolysing this waste at different temperatures (350 and 500 °C) to identify its suitability in improving the physicochemical and mechanical properties of concrete. The raw and pyrolysed forms of SCG were used as a replacement of fine aggregates (FA; sand) at 5, 10, 15 and 20% volume replacement levels. X-ray fluorescence (XRF), Carbon, Hydrogen, Nitrogen, and Sulfur (CHNS) analysis, laser diffraction particle size analysis, X-ray diffraction (XRD), scanning electron microscopy (SEM) and compressive strength tests were undertaken to investigate the properties of the raw material and their performance in the blended concrete composites. The results show that the leaching of organic compounds from the SCG hinders the hydration reaction of cement particles, thereby significantly hampering the compressive strength of SCG-blended concrete. However, pyrolysing the SCG at 350 °C led to a significant improvement in its material properties, which resulted in a 29.3% enhancement in the compressive strength of the composite concrete blended with coffee biochar.

## 1. Introduction

The disposal of organic waste poses a major environmental challenge (Oliveira et al., 2017; Roychand et al., 2021c) as it generates methane gas which is 21 times worse than CO<sub>2</sub> in its global warming potential (Melikoglu et al., 2013). In addition, the decomposition process emits several other greenhouse gases (GHGs) like carbon dioxide, nitrous oxide and ammonia (Santos et al., 2018). Spent coffee grounds (SCG) are one of the organic wastes that make up a significant proportion of the total organic waste going to landfills. Australia generates around 75,000 tonnes of ground coffee waste every year, a significant proportion of which is directly deposited into landfills. This leads to the production of methane gas, which contributes significantly to climate change (Mofijur

et al., 2020). Therefore, there is an urgent need to discover various recycling solutions that can help in diverting this waste from going to landfills into commercial applications. This transformation of waste into a resource for commercial applications can not only address the GHG emissions associated with the disposal of organic waste but would also contribute towards the closed-loop circular economy (Andrade et al., 2020; Kilmartin-Lynch et al., 2023; Kilmartin-Lynch et al., 2021b; Liu and Huang, 2018; Perera et al., 2022, 2023, Saberian et al., 2020, 2021b; Zhang et al., 2020; Zhu et al., 2022).

Parallely, the ongoing extraction of natural sand to meet the rapidly growing demands of the construction industry has significant implications for the environment and long-term sustainability. There are critical and long-lasting challenges in maintaining a sustainable supply of sand

\* Corresponding author.

\*\* Corresponding author.

E-mail addresses: [rajeev.roychand@rmit.edu.au](mailto:rajeev.roychand@rmit.edu.au) (R. Roychand), [shannon.kilmartin-lynch@rmit.edu.au](mailto:shannon.kilmartin-lynch@rmit.edu.au) (S. Kilmartin-Lynch), [mohammad.boroujeni@rmit.edu.au](mailto:mohammad.boroujeni@rmit.edu.au) (M. Saberian), [jie.li@rmit.edu.au](mailto:jie.li@rmit.edu.au) (J. Li), [kevin.zhang@rmit.edu.au](mailto:kevin.zhang@rmit.edu.au) (G. Zhang), [chunqing.li@rmit.edu.au](mailto:chunqing.li@rmit.edu.au) (C.Q. Li).

<sup>1</sup> Joint First Author, Research Fellow, School of Engineering, RMIT University, Melbourne, Victoria, Australia.

<sup>2</sup> Joint First Author, Indigenous Pre-Doctoral Research Fellow, School of Engineering, RMIT University, Melbourne, Victoria, Australia.

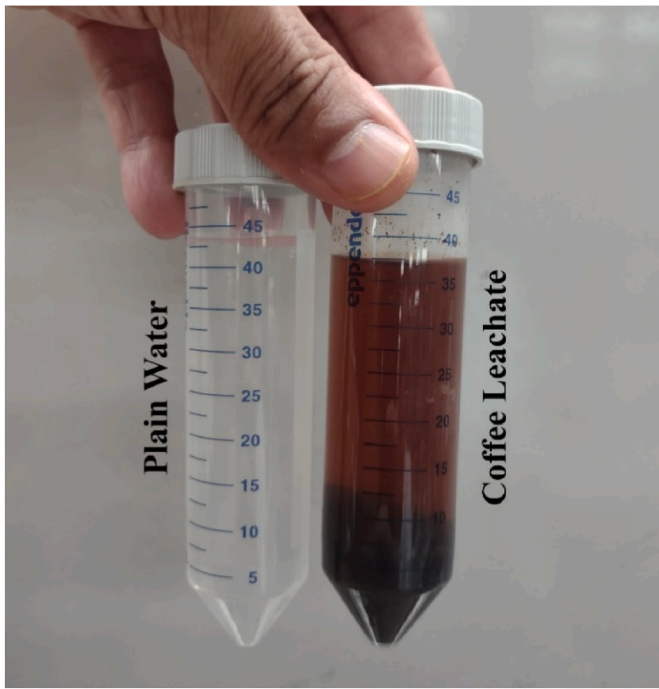


Fig. 1. Coffee leachate from SCG.

Table 1  
Concrete mix designs.

| Concrete Mix (m <sup>3</sup> ) | Cement (kg) | SCG/CBC (kg) | Water (L) | FA (kg) | 7 mm CA (kg) | 14 mm CA (kg) |
|--------------------------------|-------------|--------------|-----------|---------|--------------|---------------|
| Control                        | 350         | 0            | 214       | 820     | 450          | 535           |
| SCG05                          | 350         | 17           | 214       | 779     | 450          | 535           |
| SCG10                          | 350         | 34           | 214       | 738     | 450          | 535           |
| SCG15                          | 350         | 52           | 214       | 697     | 450          | 535           |
| SCG20                          | 350         | 69           | 214       | 656     | 450          | 535           |
| 350CBC05                       | 350         | 5            | 214       | 779     | 450          | 535           |
| 350CBC10                       | 350         | 9            | 214       | 738     | 450          | 535           |
| 350CBC15                       | 350         | 14           | 214       | 697     | 450          | 535           |
| 350CBC20                       | 350         | 19           | 214       | 656     | 450          | 535           |
| 500CBC05                       | 350         | 4            | 214       | 779     | 450          | 535           |
| 500CBC10                       | 350         | 8            | 214       | 738     | 450          | 535           |
| 500CBC15                       | 350         | 12           | 214       | 697     | 450          | 535           |

due to the finite nature of sand resources and the environmental impacts associated with sand mining. Therefore, the construction industry needs to explore alternative raw materials to ensure its long-term sustainability (Cao et al., 2022; Wang et al., 2021). The previous research shows that the concrete industry holds immense potential for significantly enhancing the utilisation of various industrial by-products and

waste materials, like fly-ash (Abhishek et al., 2022; Roychand et al., 2016a, 2016b), slag (Amran et al., 2021; Gencel et al., 2021; Roychand et al., 2018, 2020b), glass (Cao et al., 2021; Guo et al., 2020; Nodehi and Mohamad Taghvaei, 2022), tyre rubber (Abd-Elaal et al., 2019; Gill et al., 2023; Gravina et al., 2021; Islam et al., 2023; Islam et al., 2022a,b; Roychand et al., 2020a, 2021a; Youssf et al., 2019, 2020, 2022), plastic (Alqahtani and Zafar, 2021; Li et al., 2020; Maghfouri et al., 2022) and pyrolysed forms of different organic waste materials (Chen et al., 2022; Liu et al., 2022; Saberian et al., 2021a; Zhang et al., 2022a). Therefore, construction industry throws a great opportunity to increase the uptake of SCG, that would not only address the environmental concerns

Table 2  
Particle size distributions of OPC, CBC, FA and CA.

| Materials | D <sub>10</sub> | D <sub>25</sub> | D <sub>50</sub> | D <sub>75</sub> | D <sub>100</sub> |
|-----------|-----------------|-----------------|-----------------|-----------------|------------------|
| OPC       | 3.59 μm         | 4.65 μm         | 15.5 μm         | 22.5 μm         | 40.1 μm          |
| SCG       | 45.6 μm         | 163 μm          | 272 μm          | 352 μm          | 969 μm           |
| 350CBC    | 42.3 μm         | 147 μm          | 224 μm          | 324 μm          | 859 μm           |
| 500CBC    | 30.6 μm         | 126 μm          | 218 μm          | 317 μm          | 666 μm           |
| FA (Sand) | 137 μm          | 220 μm          | 347 μm          | 515 μm          | 1420 μm          |
| 7 mm CA   | 2.4 mm          | 3.5 mm          | 4.9 mm          | 5.9 mm          | 7 mm             |
| 10 mm CA  | 3.0 mm          | 5.8 mm          | 7.4 mm          | 8.5 mm          | 10 mm            |

Table 3  
CHNS analysis of SCG, 350CBC and 500CBC samples.

| Material | Carbon (weight %) | Hydrogen (weight %) | Nitrogen (weight %) | Sulfur (weight %) |
|----------|-------------------|---------------------|---------------------|-------------------|
| SCG      | 51.2 ± 0.35       | 6.89 ± 0.04         | 3.0 ± 0.12          | 0.6 ± 0.04        |
| 350CBC   | 62.8 ± 0.25       | 5.3 ± 0.02          | 3.3 ± 0.03          | 0.5 ± 0.07        |
| 500CBC   | 71.4 ± 0.33       | 2.8 ± 0.06          | 4.2 ± 0.14          | 1.3 ± 0.10        |

Table 4  
XRF analysis of SCG, 350CBC and 500CBC.

| Elements | Material Percentage Composition |        |        |
|----------|---------------------------------|--------|--------|
|          | SCG                             | 350CBC | 500CBC |
| K        | 1.0                             | 15.3   | 10.8   |
| Ca       | 0.64                            | 1.17   | 2.11   |
| Mg       | 0.08                            | 0.40   | 0.53   |
| Si       | 0.03                            | -      | 0.03   |
| P        | 0.23                            | 0.32   | 0.47   |
| S        | 0.22                            | 0.18   | 0.13   |
| Cl       | -                               | 0.15   | 0.04   |
| Mn       | 0.03                            | 0.03   | 0.07   |
| Fe       | 0.06                            | 0.07   | 0.14   |
| Ni       | 0.01                            | 0.01   | 0.01   |
| Cu       | 0.05                            | 0.04   | 0.10   |
| Zn       | 0.01                            | 0.01   | 0.04   |
| Br       | -                               | 0.03   | -      |
| Rb       | -                               | 0.04   | 0.05   |
| Sr       | 0.01                            | 0.01   | 0.03   |

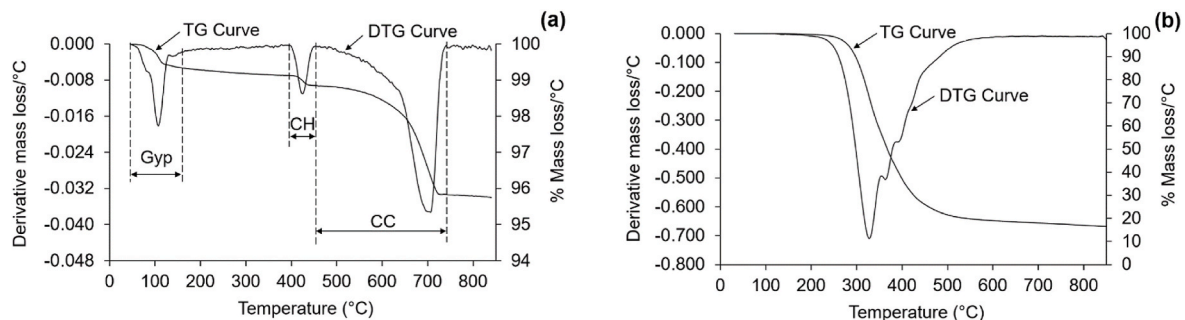


Fig. 2. TGA and its DTG mass loss curves of (a) OPC and (b) SCG.

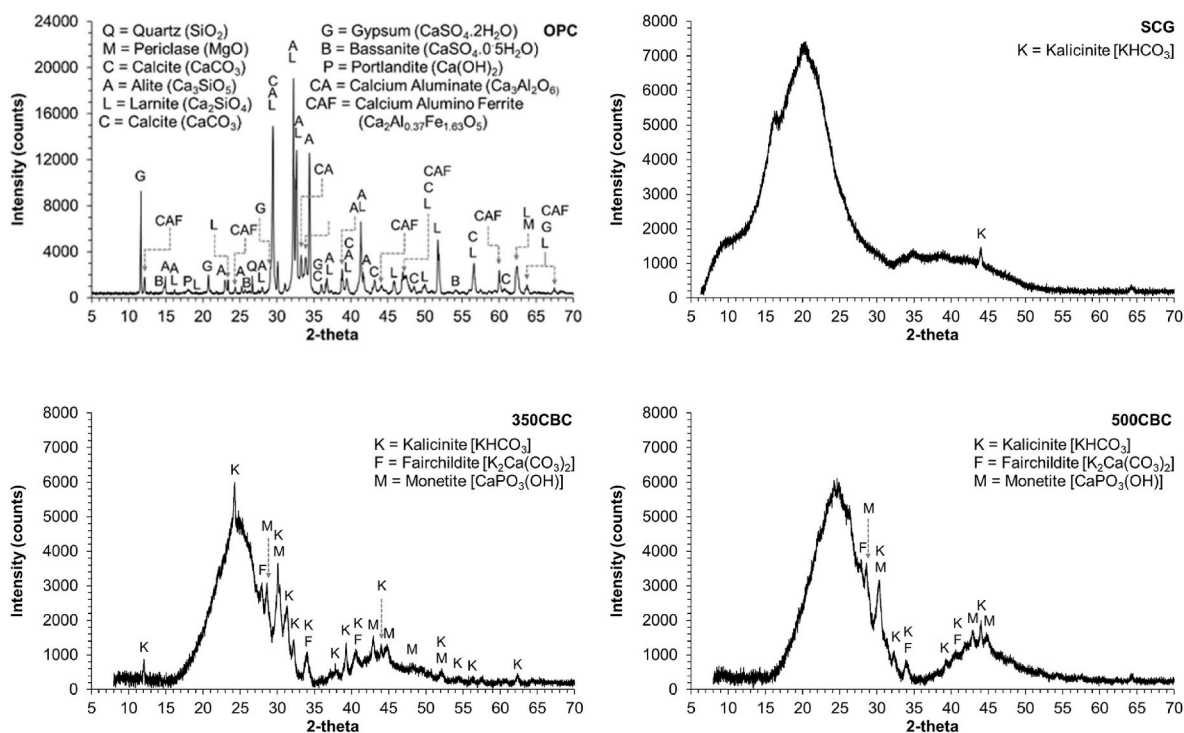


Fig. 3. XRD analysis of OPC, SCG, 350CBC and 500CBC.

associated with its disposal in landfills but could also contribute to the reduction of the continuous mining of natural resources for concrete production.

Due to its fine particle size, SCG have been researched for a few civil and construction applications (Arulrajah et al., 2016, 2017; Jalkh et al., 2018; Muñoz Velasco et al., 2016). Mohamed and Djamila (2018) looked at the mechanical properties of dune sand concrete containing SCG as a replacement of fine aggregate (FA). SCG were introduced into the control mix at rates of 5, 10, 15 and 20% to replace FA. The study determined that the compressive and flexural strengths of the concrete containing SCG were significantly impacted, with results showing a decrease in strength of 44% and 68% at 20% FA replacement, respectively, at 28 days of testing whilst also reducing the workability of the concrete by approximately 77%. Eliche-Quesada et al. (2011) conducted studies on varying waste forms in the production of ceramic bricks; it was noted throughout the study that the utilisation of SCG increased the water-absorption of the ceramic bricks; however, the inclusion of SCG impacted the compressive strength and thermal conductivity. Similarly, Sena da Fonseca et al. (2014) studied the effect of different clay and SCG mixes in ceramics by using SCG as an additive. SCG were mixed into a clay paste at 5, 10, 15 and 20% by material weight. The experiment noted that an increase in SCG showed a significant reduction in the rupture modulus. The study demonstrated that the incorporation of 5% SCG resulted in a reduction of strength by more than 30%. The relationship between the amount of SCG and the reduction in strength was found to be linear. Also, the thermal-conductivity decreased by up to 70% across samples containing SCG.

In a natural state, SCG are not a suitable replacement for construction materials. However, consequent studies have found that altering the state of SCG can show positive results for use in construction applications. Na et al. (2021) studied the effect of SCG-derived activated carbon on the compressive strength of mortar samples. The collected SCG underwent a physical activation process, which converted them into activated-carbon granules. The initial results of the study demonstrated that the addition of activated carbon up to 1.5 percent by weight of cement led to an incremental increase in the compressive strength of cement mortars. However, more significant amounts >5%wt of cement

substantially decreased compressive strength.

The application of organic waste biochar in concrete has recently been gaining a lot of research attention for carbon sequestration of organic waste and enhancement in the mechanical properties of concrete (Gupta and Kua, 2017; Gupta et al., 2018, 2021, 2022; Hu et al., 2021; Roychand et al., 2023a, 2023b; Suarez-Riera et al., 2020; Tan et al., 2021; Zhang et al., 2022b). The compressive strength of cement mortar and concrete containing biochar is dependent on the water-to-cement ratio, curing conditions and the type and amount of biochar used. It is widely accepted that optimising the amount of biochar added to the mixture improves its mechanical properties. In a research conducted by Gupta et al. (2018), various levels of cement replacement using mixed wood sawdust biochar (1%, 2% and 5%) were tested to evaluate their effect on the strength of mortar. The findings revealed that the optimum amount of mixed-wood sawdust biochar as a partial cement replacement of cement is 1%. When the dosage of mixed-wood sawdust biochar is increased up to 5%, the 28-day strength of the mixture decreases by 10%–15% compared to the optimal amount. Besides the concentration, the type of biochar used also affects the compressive strength of biochar blended cement composites. The study discovered that mortar mixed with mixed wood sawdust biochar demonstrated better compressive strength than that mixed with food waste biochar and rice waste biochar (Gupta et al., 2018). This difference was ascribed to mixed-wood sawdust biochar having higher pore structure and surface area.

Gupta et al. (2020) studied the effects of wood-based biochar on the mechanical and permeability properties of cement concrete after being exposed to elevated temperatures. The study demonstrated an improvement in water tightness and mechanical strength compared to the control sample. A 0.50% addition of the wood-based biochar by weight of cement resulted in an increase of 17% and 16% at 7-day and 28-day intervals, respectively, compared to the control sample. The improvements in compressive strength were noted down to increased densification and water tightness because of the biochar addition. Similarly, Cuthbertson et al. (2019) researched biochar derived from residual biomass as a filler material in concrete to improve its thermal and acoustic properties. The biochar utilised in the experiment was

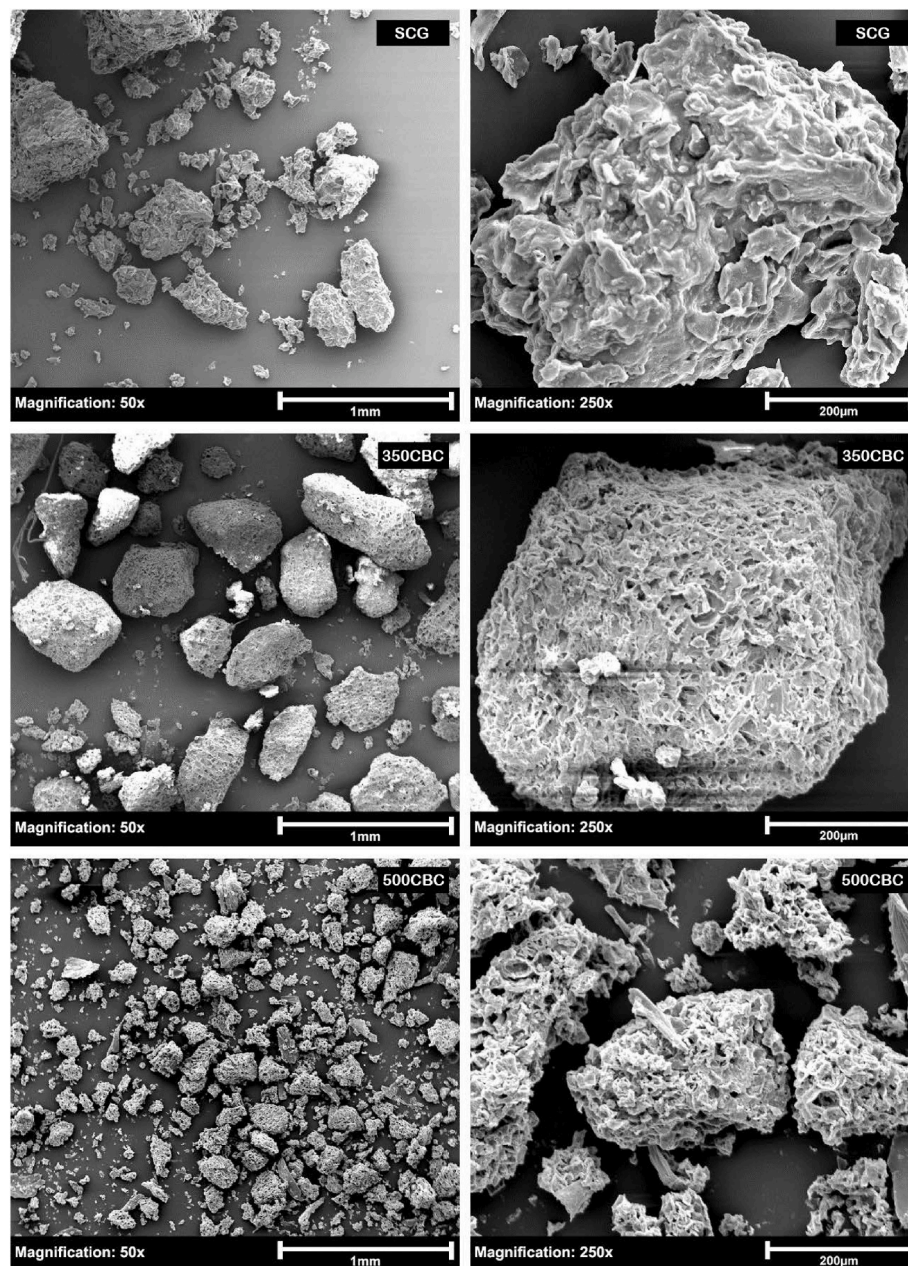


Fig. 4. SEM images of SCG, 350CBC and 500CBC at 50x and 250x magnification levels.

sourced from the raw feedstock. The study concluded that the increase in biochar content resulted in a reduction in the corresponding density of the concrete composite. Moreover, the inclusion of biochar enhanced the thermal insulation properties of the concrete when compared to the control sample, with the thermal-conductivity of the concrete being more favourable at 1% & 2% biochar by weight of concrete.

To the best of the authors' knowledge, there is no study available on the application of pyrolysed forms of SCG thermally treated at different temperatures as a replacement of FA in concrete. The potential application of treated SCG in concrete can help in preserving the invaluable natural resources that must be continuously mined to satisfy the expanding demand in the construction sector. Therefore, to address this research gap, a comprehensive study was undertaken on the raw and pyrolysed forms of SCG thermally treated at 350 and 500 °C temperatures for its application in concrete as a replacement of FA at 5, 10, 15 and 20 vol% replacement levels. Detailed physicochemical, mechanical and microstructure studies were undertaken on the raw material and

SCG/biochar blended concrete composites. X-ray fluorescence (XRF); Carbon, Hydrogen, Nitrogen and Sulfur (CHNS) analysis; laser diffraction particle size analysis; X-ray diffraction (XRD) and scanning electron microscopy (SEM); and compressive strength tests were undertaken to investigate the properties of the raw material and their performance in the blended concrete composites containing different concentrations of raw and pyrolysed forms of the SCG.

## 2. Experimental programme

### 2.1. Materials, mix designs and methods

#### 2.1.1. Materials

The materials used in this experimental program were Eureka ordinary Portland cement (OPC), SCG, SCG biochars, coarse aggregate (CA), FA and water. SCG were collected from various café retailers in Melbourne, Australia and dried in an oven for 48 h at 60 °C until no further

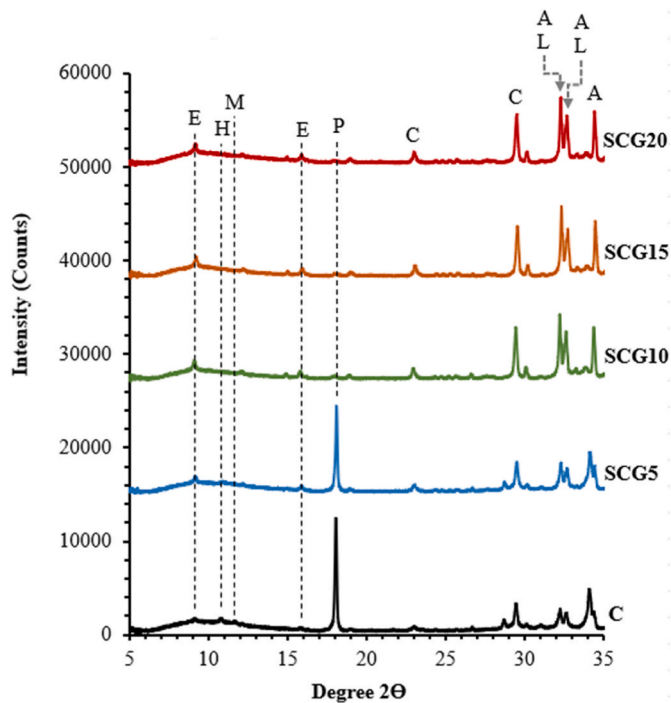


Fig. 5. XRD analysis of cement paste containing different concentrations of SCG. Note: E = Ettringite [Ca<sub>3</sub>Al<sub>2</sub>O<sub>6</sub>·3CaSO<sub>4</sub>·32H<sub>2</sub>O]; H=Hemicarbonate [Ca<sub>3</sub>Al<sub>2</sub>O<sub>6</sub>·0.5CaCO<sub>3</sub>·12H<sub>2</sub>O]; M = Monocarbonate [Ca<sub>3</sub>Al<sub>2</sub>O<sub>6</sub>·CaCO<sub>3</sub>·11H<sub>2</sub>O ]; P=Portlandite[Ca(OH)<sub>2</sub>]; C=Calcite[CaCO<sub>3</sub> ]; A = Alite [Ca<sub>3</sub>SiO<sub>5</sub>]; L = Larnite[Ca<sub>2</sub>SiO<sub>4</sub>].

loss in moisture was observed (complete drying) before using it in its raw form in concrete. The SCG biochars were produced at two different temperatures of 350 and 500 °C. The specific gravity of OPC (SG = 3.1) was obtained from the cement manufacturer. The specific gravities of the remaining materials were calculated using the volume displacement method. All the different materials were soaked in water to fill in the pore structure. A small 10 mL (25 mL for CA) graduated cylinder partially filled with a known vol/wt of water was used to identify the increase in the volume of water with the addition of saturated surface dried material. The material was dried in an oven at 60 °C for the complete elimination of water from the pore structure to identify the dry weight of the sample. The specific gravity of the materials was calculated using the known volume and dry weight of the material. The specific gravities of SCG, 350CBC and 500CBC were 1.1, 0.3 and 0.265, respectively, and that of FA and CA were 2.62 and 2.73, respectively.

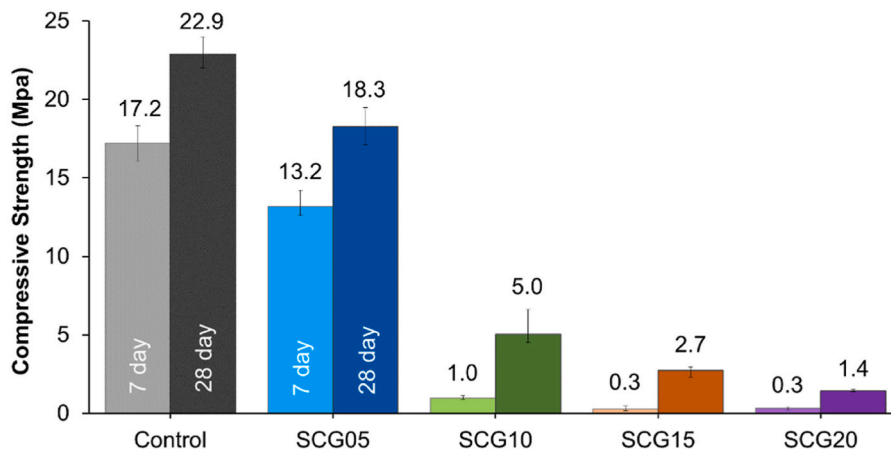


Fig. 6. Compressive strength results for SCG at 7 and 28-days.

2.1.2. Leaching test for SCG

Leaching test was conducted on SCG to detect if they leach out organic compounds that may influence the hydration reaction of cement particles. A small amount of SCG was soaked in water in a test tube for 5 min with continuous shaking to provide a high shear mixing as provided to the concrete mix. Fig. 1 shows that the colour of the water changed to brown due to the leaching of organic compounds from the SCG.

2.1.3. Preparation of coffee biochar (CBC)

The SCG were collected from different cafeterias and filled into the aluminium trays. An aluminium foil was wrapped tight on top of the tray to seal it from all sides. Small micro holes were pierced into the aluminium foil at random locations to allow for the escape of gases during the thermal decomposition of SCG. The SCG were then pyrolysed at 350 and 500 °C temperatures for 2 h each at the heating rate of 10 °C/min in Barnstead Thermolyne Furnace Type 30400. The furnace was

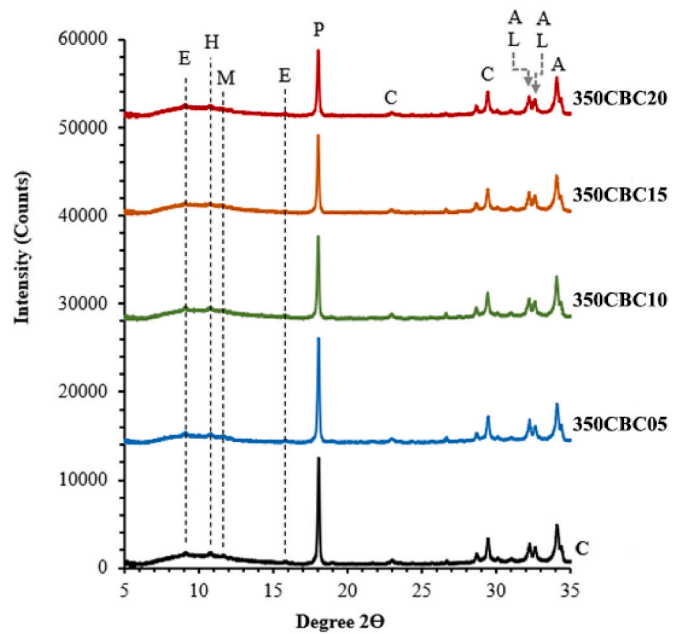


Fig. 7. XRD analysis of cement paste containing different concentrations of 350CBC

Note: E = Ettringite [Ca<sub>3</sub>Al<sub>2</sub>O<sub>6</sub>·3CaSO<sub>4</sub>·32H<sub>2</sub>O]; H=Hemicarbonate [Ca<sub>3</sub>Al<sub>2</sub>O<sub>6</sub>·0.5CaCO<sub>3</sub>·12H<sub>2</sub>O]; M = Monocarbonate [Ca<sub>3</sub>Al<sub>2</sub>O<sub>6</sub>·CaCO<sub>3</sub>·11H<sub>2</sub>O ]; P=Portlandite[Ca(OH)<sub>2</sub>]; C=Calcite[CaCO<sub>3</sub> ]; A = Alite [Ca<sub>3</sub>SiO<sub>5</sub>]; L = Larnite[Ca<sub>2</sub>SiO<sub>4</sub>].

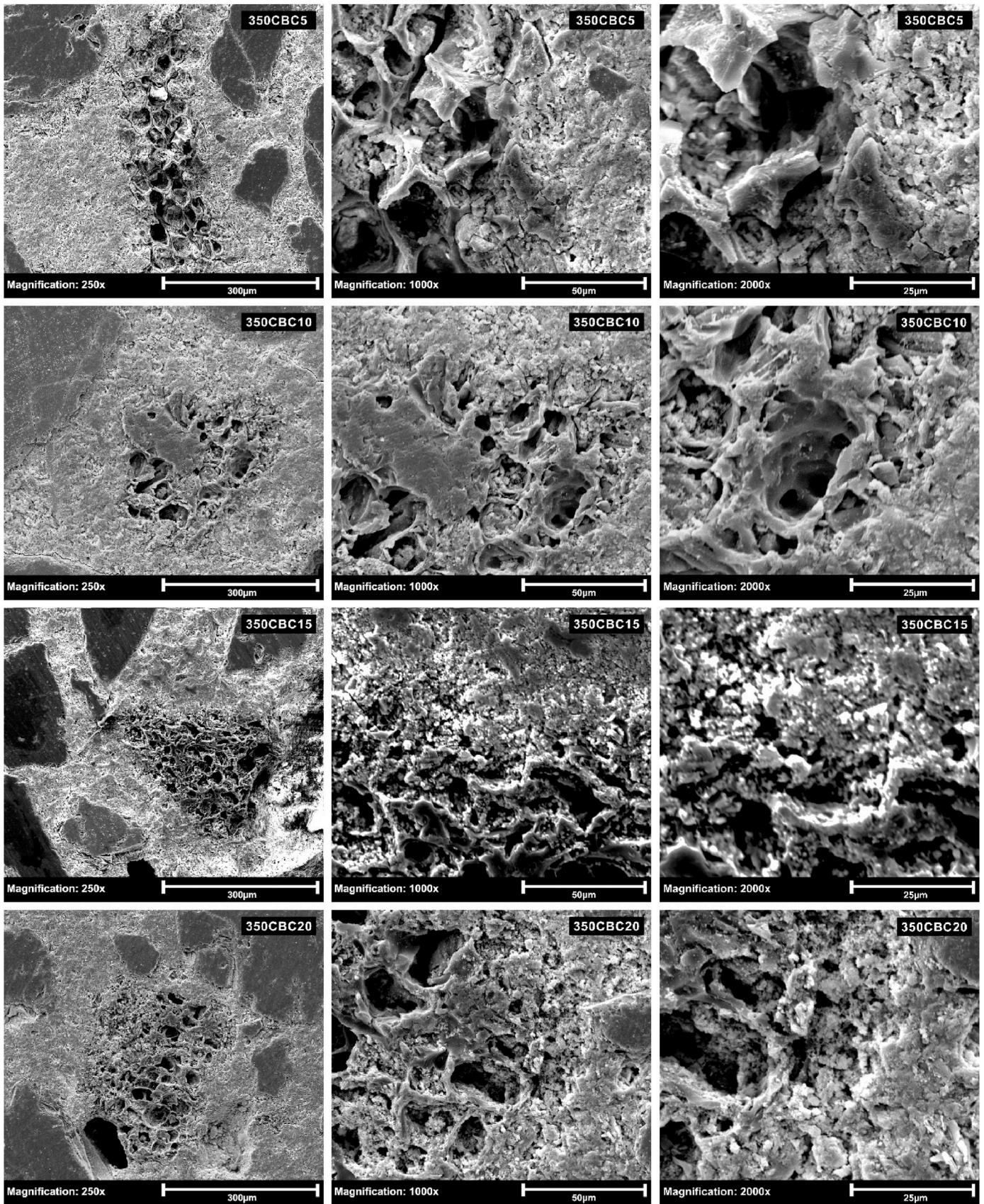


Fig. 8. SEM images of 350CBC concrete samples.

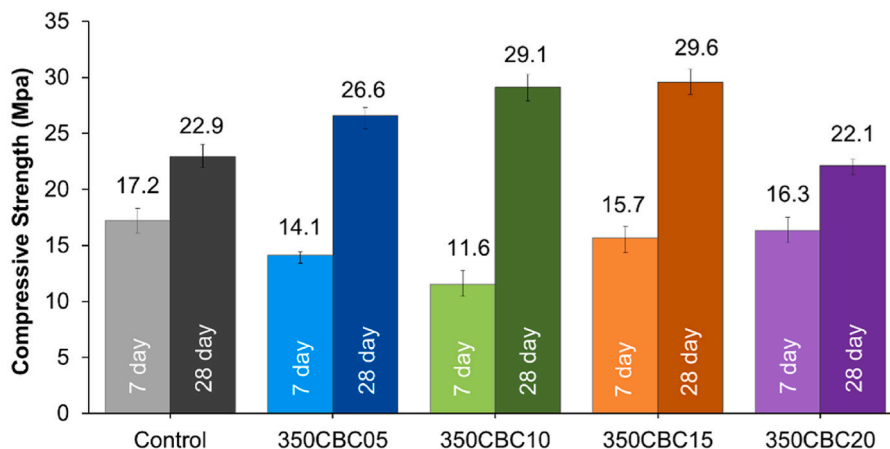


Fig. 9. Compressive strength results of 350CBC.

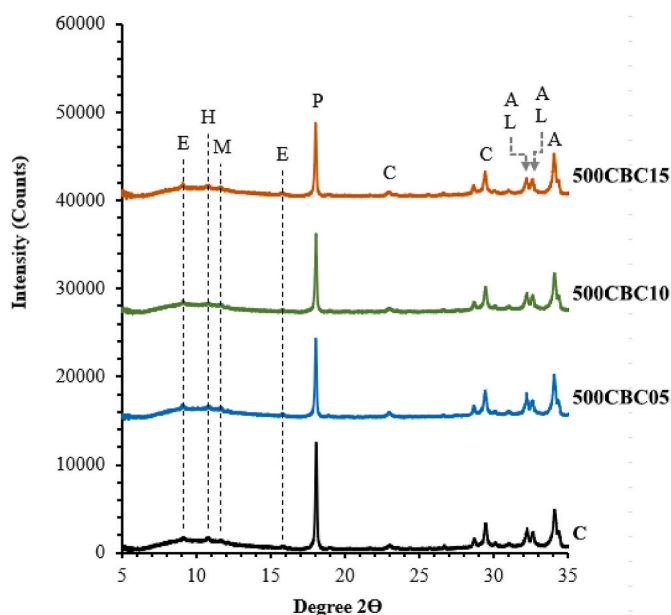


Fig. 10. XRD analysis of cement paste containing different concentrations of 500CBC.

Note: E = Ettringite [ $\text{Ca}_3\text{Al}_2\text{O}_6 \cdot 3\text{CaSO}_4 \cdot 32\text{H}_2\text{O}$ ]; H=Hemicarbonate [ $\text{Ca}_3\text{Al}_2\text{O}_6 \cdot 0.5\text{CaCO}_3 \cdot 12\text{H}_2\text{O}$ ]; M = Monocarbonate [ $\text{Ca}_3\text{Al}_2\text{O}_6 \cdot \text{CaCO}_3 \cdot 11\text{H}_2\text{O}$ ]; P=Portlandite [ $\text{Ca}(\text{OH})_2$ ]; C=Calcite [ $\text{CaCO}_3$ ]; A = Alite [ $\text{Ca}_3\text{SiO}_5$ ]; L = Larnite [ $\text{Ca}_2\text{SiO}_4$ ].

allowed to cool down before removing the residual biochar. The SCG biochar produced at 350 °C was nominated as 350CBC, and that produced at 500 °C was nominated as 500CBC. The 350CBC and 500CBC coffee biochars were produced in bulk, which were further used in the concrete mix designs at different sand replacement levels of 5, 10, 15 and 20 vol% (350CBC05, 350CBC10, 350CBC15, 350CBC20, 500CBC05, 500CBC10 and 500CBC15).

## 2.2. Mix designs

Twelve mix designs were utilised to compare the effects of SCG in the forms of untreated SCG, 350-degree biochar and 500-degree biochar on the mechanical and microstructural behaviour of concrete. Four were used as regular SCG, four at 350° and a further four at 500°, considering the varying specific gravity of the material at the respective temperatures. The untreated SCG and biochars were then incorporated at rates of

0%, 5%, 10%, 15% and 20 vol% (to act as a substitute for FA. Table 1 details all mix proportions utilised throughout the experimental study on CBC and the varying percentages that the biochars and SCG were incorporated as a substitute for FA. For instance, SCG10 denotes that 10% SCG was included as a FA replacement; 350CBC05 indicates that the CBC was produced at 350 °C and incorporated at a rate of 5% (by FA replacement), whereas 500CBC05 similarly represents CBC made at 500 °C at a rate of 5% FA replacement. The mix proportions for 350-degree and 500-degree CBC differ only slightly due to the small difference in the specific gravity of the two materials.

## 2.3. Casting and curing

All concrete specimens were prepared for compressive strength test throughout the casting procedure by following AS 1012.8.1 (2014). Due to the loss in weight and volume of producing biochar from SCG, smaller moulds were utilised for compressive strength testing at sizes 75 mm (D) x 150 mm (H). For casting purposes, a cement paste was formed in the concrete mixer by combining cementitious materials and water to decrease the formation of lumps throughout the mixing process. After the cement paste was formed, CBC were prepared at 350 and 500°, and SCG were separately added to the mixer to allow for a better distribution of materials. Finally, FA and CA were added into the mix and mixed for 3 min to allow for a uniform distribution of materials. The fresh concrete was poured into the lubricated moulds and vibrated to remove any air pockets. The samples were cured at room temperature for 24 h, demoulded and cured in a water tank at approximately 22 °C until the time of testing (El-Hassan et al., 2021; Roychand et al., 2021b). Similar methods to casting and curing were utilised in previous studies (Kil-martin-Lynch et al., 2021a, 2022; Roychand et al., 2021a). The samples were ground flat at the top to eliminate rough surface that can potentially create stress concentration points prior to carrying out the compressive strength tests.

## 2.4. Testing procedures

### 2.4.1. Compressive strength test

Compressive strength testing on the concrete samples was conducted under AS 1012.9 (2014), utilising the Materials Testing System (MTS) equipment. Due to the size of the compressive strength samples, a loading rate of 88 kN/min was applied.

### 2.4.2. XRD analysis

The XRD analysis was carried out on cement paste specimens containing different concentrations of SCG, 350CBC and 500CBC. The concentrations were kept the same as shown in the mix design (Table 4);

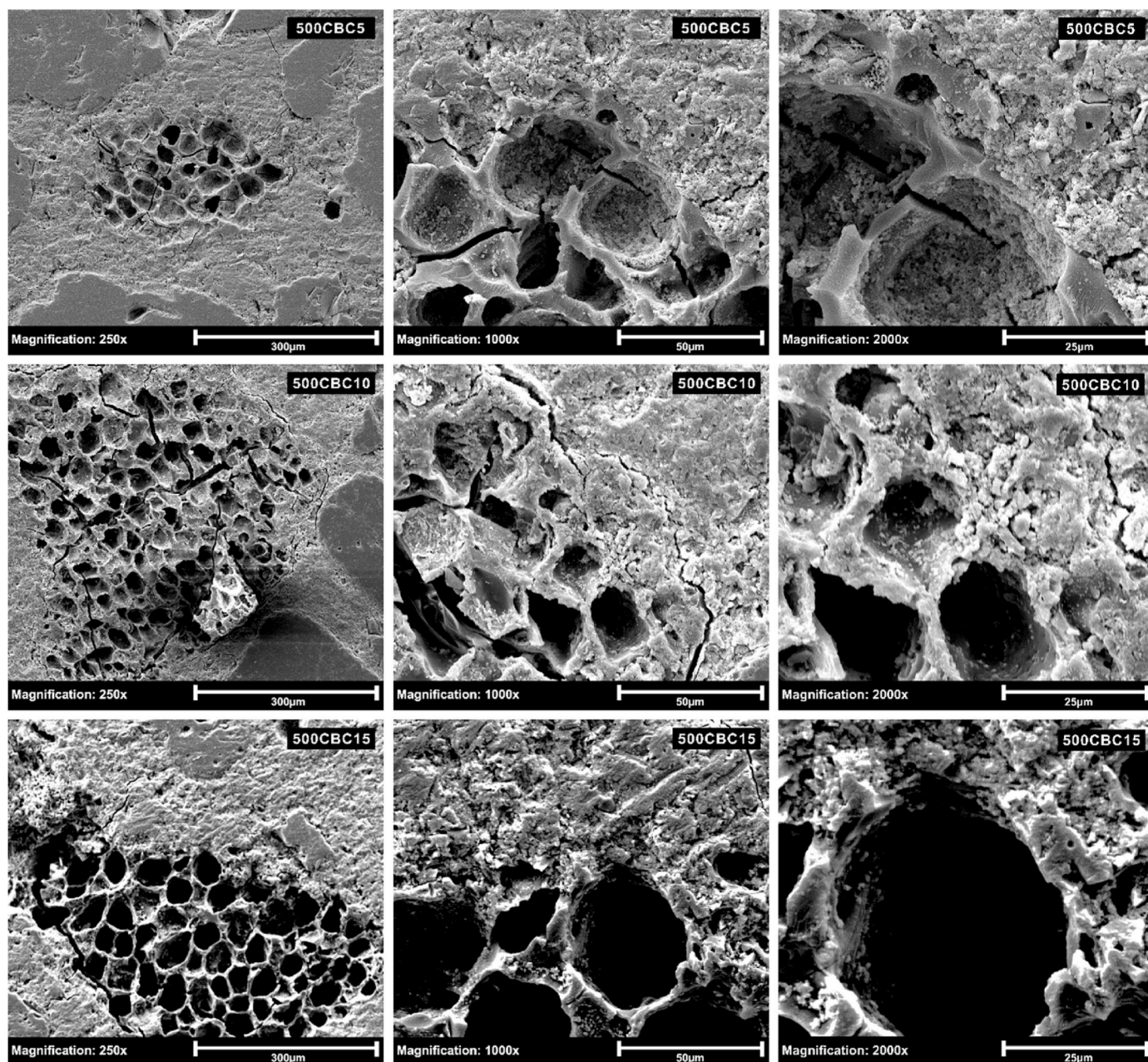


Fig. 11. SEM images of 500CBC concrete samples.

however, the inert sand and CA were not incorporated to ascertain the effect of SCG, 350CBC and 500CBC on the hydration reaction of cement.

#### 2.4.3. SEM analysis

The SEM analysis of the concrete specimens containing SCG, 350CBC and 500CBC was carried out using FEI Quanta200SEM to ascertain the properties of cement microstructure and the bond performance of the SCG and biochars with the cement matrix. The concrete samples containing SCG had very low strength, due to which grinding and polishing were not possible. Therefore, the SEM analysis was carried out only on the 350CBC and 500CBC biochar blended concrete samples.

### 3. Experimental results and discussion

#### 3.1. Material properties

##### 3.1.1. Thermogravimetric analysis of SCG

Thermogravimetric analysis (TGA) of OPC and SCG was carried out using PerkinElmer STA8000 equipment in a  $N_2$  environment at  $N_2$  flow rate of 20 mL/min. The TGA and differential thermogravimetry (DTG) mass loss curves of OPC and SCG are shown in Fig. 2. The TGA analysis of OPC shows the presence of Gypsum, Bassanite, Calcium Hydroxide (CH) and Calcium Carbonate (CC). The concentration of CH was 1.15%, and that of CC was 6.85%. The TGA analysis of dried coffee grounds starts at  $\sim 135^\circ C$  and ends at  $\sim 575^\circ C$  temperature. After the complete thermal decomposition of coffee grounds, the residual inorganic material is  $\sim 16.4\%$  of the original mass of the dried coffee grounds.



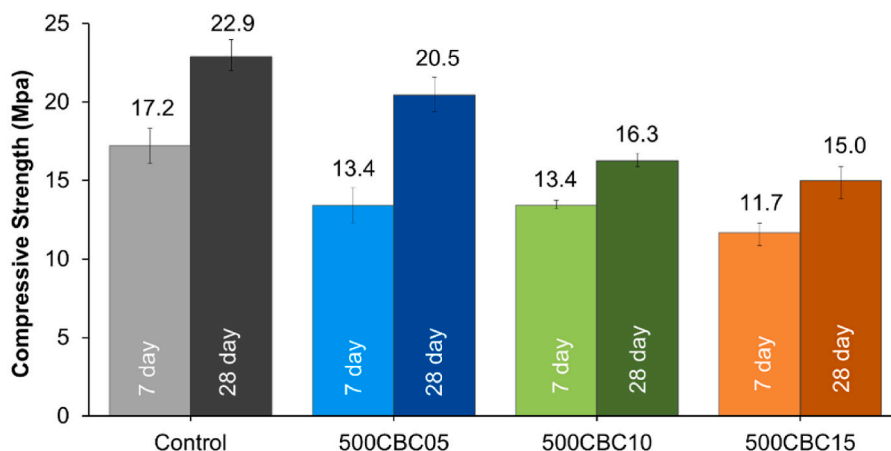


Fig. 12. Compressive strength results for 500CBC.

### 3.1.2. Particle size distribution (PSD)

The PSD of OPC, SCG, 350CBC, 500CBC and sand was undertaken using the Malvern particle size analyser “Malvern Mastersizer 3000”, and that of CA was carried out using the sieve-analysis (Table 2).

### 3.1.3. CHNS analysis of SCG, 350CBC, 500CBC

The CHNS analysis, as shown in Table 3, was carried out on the SCG and the CBC specimens using PerkinElmer Series II CHNS analyser.

### 3.1.4. Elemental composition of SCG, 350CBC, 500CBC

The elemental compositions (Table 4) of SCG and the biochar samples were identified using the Bruker-AXS-S4-Pioneer XRF equipment.

### 3.1.5. XRD of OPC, SCG, 350CBC and 500CBC

The XRD analysis of dried and finely ground OPC, SCG, 350CBC and 500CBC samples was carried out using the solvent exchange method (Roychand, 2017; Roychand et al., 2018). The XRD data were collected between 5° and 70° 2theta using a step size of 0.1° and a count time of 0.5sec per step to ascertain their mineralogical composition. Fig. 3 shows the different mineralogical compositions of OPC, SCG, 350CBC and 500CBC samples. SCG shows amorphous broad humps centred around 20 and 38° 2theta locations. These amorphous humps are more likely from the organic phases present in the SCG. These amorphous humps shift to higher 2theta angles (i.e., 25 and 45° 2theta) due to the thermal decomposition of organic compounds into residual carbon.

### 3.1.6. SEM analysis of SCG, 350CBC and 500CBC

SEM analysis of SCG, 350CBC and 500CBC was carried out using FEI-Quanta200ESEM at 50x and 250x magnification levels (Fig. 4) for the visual identification of their surface microstructure characteristics. Coffee ground particles show solid microstructure; however, the thermal decomposition of coffee grounds due to pyrolysis created a porous structure within the particles that increased with the increase in the pyrolysis temperature.

## 3.2. Effect of SCG on concrete properties

### 3.2.1. XRD analysis

XRD analysis of cement paste samples containing different concentrations of SCG (Fig. 5) shows that the portlandite content decreases considerably with the addition of 5% of SCG. With the further increase in the concentration of SCG, there is a drastic reduction in the portlandite ( $\text{Ca}(\text{OH})_2$ ) content, which is close to negligible content. This is followed by an increase in the ettringite, calcite, alite and larnite phases. The increase in Alite and Larnite phases with the increase in SCG content shows that the addition of SCG significantly hampers the hydration

reaction of calcium silicate phases. The organic compounds leached by the SCG (Fig. 1) are most likely instrumental in hindering the hydration reaction of cement particles.

Calcium carbonate takes part in the hydration reaction to produce hemi-carboaluminate, mono-carboaluminate and other carbonate phases. With the hindering of the hydration of cement particles, the calcium carbonate present in OPC stays unreacted; therefore, this content increases with the increase in SCG concentration. Interestingly, the ettringite peaks show an increase in intensity with the increase in SCG. This indicates that the reaction of calcium aluminate and gypsum phases is promoted by the SCG.

### 3.2.2. Compressive strength results of SCG at 7 and 28 days

Fig. 6 details the compressive-strength results at 7 and 28 days of blended concrete composites containing different concentrations of SCG incorporated as a replacement of FA by volume. It can be noted that the compressive strength of concrete decreases with the increase in the percentage of SCG. The XRD and the SCG leachate analyses show that the addition of SCG releases the organic compounds that are hindering the hydration reaction of cement particles, which increases with the increase in SCG content. This hindrance in the hydration reaction of the cement particles by the organic compounds leaching from SCG is instrumental in negatively affecting the compressive-strength results of SCG concrete. Similar reductions in the compressive-strength results with the incorporation of organic waste into cement composites/concrete have been reported by other authors like Sena da Fonseca et al. (2014), who reported the negative effects of the incorporation of SCG in cement composites and Roychand et al. (2021c) who reported the negative effects of incorporating untreated biosolid waste in cement composites.

## 3.3. Effect of 350CBC on concrete properties

### 3.3.1. XRD analysis

Fig. 7 shows the XRD diffractograms of hydrated cement paste specimens containing different concentrations of 350CBC. Interestingly, the peak intensities of Alite and Larnite phases show significant reduction compared to that of the SCG samples. This indicates that the thermal decomposition of the organic compounds due to the pyrolysis process is highly beneficial in negating the negative effects of SCG in concrete.

The XRD analysis shows that the portlandite peak intensity shows a small reduction with the addition of 350CBC, which progressively reduces with the increase in 350CBC content. The remaining peaks do not show any noticeable difference. As XRD works on a volume basis, the overall volume of the finely ground samples of hydrated cement paste

**Table 5**  
Overall summary of results.

| Test   | Results   |
|--|---|
| Coffee leaching test                                 | SCG leach organic compounds when soaked in water  |
| TGA of SCG   | The thermal decomposition of SCG takes place between ~200 and ~550 °C temperature range (Fig. 2b)   |
| Particle size distribution of SCG, 350CBC and 500CBC | SCG, 350CBC and 500CBC are finer than conventional sand   |
| CHNS analysis of SCG, 350CBC and 500CBC              | The carbon content increases with the increase in the pyrolysis temperature.  |
| XRF analysis of SCG, 350CBC and 500CBC               | A significant increase in the alkali elements like K, Ca and Mg was observed in 350CBC and 500CBC due to the thermal breakdown of the organic compounds after the pyrolysis process.  |
| XRD analysis of SCG, 350CBC and 500CBC               | SCG are overall amorphous in nature; however, their thermal decomposition at 350 and 500 °C temperatures bring about prominent crystalline peaks of kalicinite, Fairchildite and Monetite minerals.   |
| XRD analysis of SCG in concrete                      | The portlandite content decreases considerably with the addition of 5% of SCG. With the further increase in the concentration of SCG, there is a drastic reduction in the portlandite (Ca(OH) <sub>2</sub> ) content, which is close to negligible content. This is followed by an increase in the ettringite, calcite, alite and larnite phases. The increase in Alite and Larnite phases with the increase in SCG content shows that the addition of SCG significantly hampers the hydration reaction of calcium silicate phases. |
| Compressive Strength results of SCG in concrete      | The compressive strength of concrete decreases with the increase in the percentage of SCG.  |
| XRD analysis of 350CBC in concrete                   | The portlandite peak intensity shows a small reduction with the addition of 350CBC, which progressively reduces with the increase in 350CBC content. The remaining peaks do not show any noticeable difference. The reduction in the XRD peak intensities of portlandite is most likely due to the reduction in the overall OPC content in the cement paste samples modified with 350CBC. The addition of CBC does not have any influence on the chemical changes within the cement microstructure.                                 |
| SEM analysis of 350CBC in concrete                   | The SEM images show that the biochar has an excellent bond performance with the cement matrix. It can also be noted that the cement paste has penetrated the porous biochar material, allowing for strength development across 350CBC.  |
| Compressive Strength results of 350CBC in concrete   | The compressive-strength results of 350CBC blended concrete composites increase with the increase in 350CBC concentration of up to a maximum sand replacement level of 15%. With a further increase in the replacement level, the compressive strength starts dropping. However, even at a replacement level of 20%, the compressive strength results are somewhat at par with that of the control mix.   |
| XRD analysis of 500CBC in concrete                   | Similar to 350CBC, the XRD analysis of cement paste samples containing different concentrations of 500CBC shows a small reduction in the portlandite peak intensities that progressively decreases with the increase in 500CBC content. This is most likely because of the overall reduction in the OPC content with the increase in the proportion of 500CBC. The remaining peaks, like that of ettringite, hemi-carboaluminate, mono-carboaluminate, calcite, alite and larnite, did not show any noticeable difference.          |
| SEM analysis of 350CBC in concrete                   | The SEM images show that the biochar has an excellent bond performance with the cement matrix. However, compared to the 350CBC concrete samples, 500CBC shows highly porous biochar with extensive micro-cracking within and the areas surrounding the biochar samples. This  |

**Table 5 (continued)**

| Test   | Results   |
|--|---|
| Compressive Strength results of 500CBC in concrete | could potentially be due to the biochar skeleton structure getting fragile due to extensive thermal breakdown at a higher temperature. Across both 7-day and 28-day strength results, a decreasing trend can be seen forming throughout all mix designs from the control mix. At its lowest point, 500CBC15 denotes a decrease in strength of 34.5% compared to that of the control mix. Higher porosity and increased micro-cracking in 500CBC concrete are most likely weakening the cement microstructure, resulting in the reduction in the compressive-strength results that decrease with the increase in 500CBC content. |
| Optimised mix design                               | 350CBC15 provides the best-performing concrete mix that provides the highest improvement in the 28-day concrete strength results  |

containing different concentrations of 350CBC will have a lower concentration of OPC content with the progressive increase in 350CBC. The reduction in the XRD peak intensities of portlandite is most likely due to the reduction in the overall OPC content in the cement paste samples modified with 350CBC. Since the XRF and XRD analyses of 350CBC do not show the presence of any amorphous silica or aluminosilicates, there is no potential for the reduction of portlandite due to the pozzolanic reaction. This shows that the addition of CBC does not have any influence on the chemical changes within the cement microstructure.

### 3.3.2. SEM analysis

The SEM images showing the bond performance of 350CBC particles with the cement matrix at 250x, 1000x and 2000x magnification levels are presented in Fig. 8. The SEM images show that the biochar has an excellent bond performance with the cement matrix. It can also be noted that the cement paste has penetrated the porous biochar material, allowing for strength development across 350CBC. Moreover, biochars absorb water and contribute to the internal curing of cementitious materials once the relative internal humidity begins to drop.

### 3.3.3. Compressive strength results of CBC produced at 350 °C

It can be seen that the compressive-strength results (Fig. 9) of 350CBC blended concrete composites increase with the increase in 350CBC concentration of up to a maximum sand replacement level of 15%. With a further increase in the replacement level, the compressive strength starts dropping. However, even at a replacement level of 20%, the compressive strength results are somewhat at par with that of the control mix. Biochars have the capacity to store water within their porous microstructure. This water retained within their microstructure is released when the internal relative humidity of the cement matrix drops, providing internal curing and thereby contributing to the development of its compressive strength (Dixit et al., 2019; Gupta et al., 2018). Similar results in the improvement in compressive-strength results with the addition of wood biochar have been reported by Tan et al. (2021) and Gupta et al. (2018); however, they used wood biochar material as a very low percentage of cement replacement material.

Comparing the compressive-strength results of 350CBC with that of SCG concrete samples, it can be clearly identified that pyrolysing the SCG at 350 °C to produce 350CBC improves its material properties, which is reflected in the significant enhancement in the compressive-strength results of 350CBC concrete.

## 3.4. Effect of 500CBC on concrete properties

### 3.4.1. XRD analysis

Fig. 10 shows the XRD diffractograms of hydrated cement paste samples containing different concentrations of 500CBC. Similar to 350CBC, the XRD analysis of cement paste samples containing different

concentrations of 500CBC shows a small reduction in the portlandite peak intensities that progressively decreases with the increase in 500CBC content. This is most likely because of the overall reduction in the OPC content with the increase in the proportion of 500CBC. The remaining peaks, like that of ettringite, hemi-carboaluminate, mono-carboaluminate, calcite, alite and larnite, did not show any noticeable difference. This indicates that the different pyrolysing temperatures (350 and 500 °C) of SCG do not have any effect on the chemical reaction of cement particles.

#### 3.4.2. SEM analysis

Fig. 11 demonstrates the SEM images of the bond performance between both 500CBC and the cement matrix at 250x, 1000x and 2000x magnification levels. The SEM images show that the biochar has an excellent bond performance with the cement matrix. However, compared to the 350CBC concrete samples, 500CBC shows highly porous biochar with extensive micro-cracking within and the areas surrounding the biochar samples. This could potentially be due to the biochar skeleton structure getting fragile due to extensive thermal breakdown at higher temperature (i.e., 500 °C). This fragility is most like more dominant than the internal curing it is providing to the cement microstructure.

#### 3.4.3. Compressive strength results of CBC produced at 500 °C

The results of the 7-day and 28-day compressive-strength tests of CBC at 500° are outlined in Fig. 12. Across both 7-day and 28-day outcomes, a decreasing trend can be seen forming throughout all mix designs from the control mix. At its lowest point, 500CBC15 denotes a decrease in strength of 34.5%. As detailed in the SEM analysis, 500CBC is more porous and highly fragile compared to that of 350CBC, as evident from the extensive micro-cracking within and areas surrounding the biochar particles. Therefore, the higher porosity and increased micro-cracking are most likely weakening the cement microstructure, resulting in the reduction in the compressive-strength results, which decreases with the increase in 500CBC content. It is worth mentioning that since there was a decreasing trend in the compressive strength results from 0 to 15% replacement levels, the sample of 500CBC20 was not prepared and tested.

### 4. Overall summary of results

Table 5 provides a summary of all the results of raw materials and the application of SCG, 350CBC and 500CBC in concrete applications.

### 5. Recycling potential of waste SCG in concrete applications

It can be noted from the analysis of the application of SCG, 350CBC and 500CBC that 350CBC provides the best performance in improving the compressive strength of the biochar blended concrete composites. The best-performing mix showing the highest improvement in compressive strength is 350CBC15.

To calculate the maximum uptake of waste SCG, we know that Australia generates around 75,000 tonnes of ground coffee waste every year. Pyrolysing this waste at 350 °C temperature would generate about 22,500 tonnes of SCG biochar (350CBC). The Annual production of cement concrete in Australia is about 72,000 million tonnes. About 40% (28.8 million tonnes) of it is FA. We found that up to 15% of replacement of FA can provide a 29.3% enhancement in concrete strength. 15% of the total FA component of concrete production in Australia is 4.32 million tonnes, which is equal to 1,630,189 m<sup>3</sup> (volume) of sand (based on an average density of 2650 kg/m<sup>3</sup>). The volume of 22,500 tonnes of 350CBC is equal to 75,000 m<sup>3</sup> (based on an average density of 300 kg/m<sup>3</sup>). This shows that 100% of waste SCG produced in Australia can be consumed if used as a replacement of FA with significant enhancement in strength properties of the SCG biochar blended concrete composites.

Environmental benefits: This project will provide an incentive for the

eco-friendly disposal of organic wastes using the pyrolysis process, which, if disposed of in landfills, generates CH<sub>4</sub>, which has 21 times more global warming potential than CO<sub>2</sub> and, if incinerated, produces a huge amount of CO<sub>2</sub> emissions. This will not only help in diverting a significant amount of organic waste going to landfills but will also reduce the reliance on the continuous mining of river sand for concrete applications.

Sustainability benefits: Making concrete by recycling pyrolysed forms of organic wastes (biochar) will reduce its reliance on the continuous mining of natural resources, making it more sustainable.

Economic benefits: This project demonstrates a large commercial market for biochar derived from organic waste for its application in concrete, generating large-scale economic benefits for the country.

Employment benefits: This solution of the transformation of organic waste into a valuable resource is a new industry in itself. It would generate direct and indirect employment for the entire supply chain in production, operation and commercial end-use in concrete applications.

### 6. Conclusions and recommendations for future work

This study investigated the effect of different pyrolysing temperatures on the physicochemical and mechanical properties of blended concrete containing different concentrations of SCG, 350CBC and 500CBC.

Pyrolysing the SCG thermally breaks down the organic content leaving behind carbon-rich porous biochar. The porosity of SCG biochar increases with the increase in the pyrolysing temperature. The addition of SCG leaches organic compounds that hinder the hydration reaction of cement particles, thereby significantly hampering the compressive strength results of SCG-blended concrete. Pyrolysing SCG at 350 °C (350CBC) significantly improved its performance in concrete. The inclusion of 350CBC provided an overall increase in the compressive strength results up to a maximum sand replacement level of 15%, which provided a 29.3% increase in the compressive strength results compared to that of the control sample. This increasing trend development of compressive strength was closely linked to (i) the excellent bond performance of 350CBC with the cement microstructure, (ii) the cement paste penetrating the biochar pores strengthening the porous structure and (iii) the internal curing provided by the water stored in the porous microstructure of 350CBC.

The higher porosity and fragile skeleton structure of 500-degree CBC showed microcracking within and areas surrounding the 500CBC biochar particles, which was instrumental in negatively hampering its compressive-strength results. However, 500CBC showed an excellent bond performance with the cement matrix, similar to that of 350CBC. 100% of waste SCG biochar (350CBC) can be utilised in Australia when used as a replacement of FA.

Based on the positive experiment results, it is recommended to carry out long-term mechanical and durability tests on 350CBC for its potential applications in the construction industry. The effects of other pyrolysing temperatures on the performance of SCG biochar in concrete need to be explored. The following mechanical and durability tests will be covered as part of future works:

- Mechanical tests: (i) flexural strength, (ii) split tensile strength, (iii) modulus of elasticity, (iv) modulus of rigidity, (v) abrasion resistance, (ix) crack resistance, (xii) impact resistance, (xiii) shrinkage/expansion test, (ix) Shear Strength Test, (x) Poisson's Ratio Test, (xi) fracture energy and toughness and (xii) fatigue life test.
- Durability tests: (i) water absorption test, (ii) porosity, (iii) chloride ion penetration test, (iv) carbonation test, (v) acid attack, (vi) sulphate attack, (vii) freeze-thaw resistance, (viii) Alkali-Silica Reactivity Test (ix) effect of seawater, (x) thermal conductivity test, (xi) electrical resistivity test, (xii) ultrasonic pulse velocity test and (xiii) acoustic properties.

## Funding

This research was supported by the RMIT University's Strategic Capability Deployment Fund in collaboration with Arup Australia P/L and Earth Systems P/L (Grant No. ECPSCDF202200035).

## CRediT authorship contribution statement

**Rajeev Roychand:** Conceptualization, Funding acquisition, Methodology, Investigation, Data curation, Formal analysis, Visualization, Writing – review & editing. **Shannon Kilmartin-Lynch:** Methodology, Investigation, Data curation, Formal analysis, Visualization, Writing – review & editing. **Mohammad Saberian:** Writing – review & editing. **Jie Li:** Funding acquisition, Supervision, Methodology, Visualization, Writing – review & editing. **Guomin Zhang:** Writing – review & editing. **Chun Qing Li:** Writing – review & editing.

## Declaration of competing interest

The authors declare that they have no known competing financial interests or personal relationships that could have appeared to influence the work reported in this paper.

## Data availability

Data will be made available on request.

## Acknowledgement

The authors gratefully acknowledge RMIT University's Strategic Capability Deployment Fund, ARUP Australia P/L and Earth systems P/L for their financial and technical support for this project. We also acknowledge the RMIT University's Rheology, X-Ray and Microscopy & Microanalysis Facilities for providing training and access to the material characterisation equipment. We would also like to extend an acknowledgement to the Indigenous owned coffee supplier "Talwali Coffee" for providing the ground coffee for this experimental study.

## References

- AS 1012.8.1, 2014. Methods of Testing Concrete - Method for Making and Curing Concrete- Compression and Indirect Tensile Test Specimens. Standards Australia, Sydney, NSW.
- AS 1012.9, 2014. Methods of Testing Concrete - Compressive Strength Tests- Concrete, Mortar and Grout Specimens. Standards Australia, Sydney, NSW.
- Abd-Elaal, E.-S., Araby, S., Mills, J.E., Youssif, O., Roychand, R., Ma, X., Zhuge, Y., Gravina, R.J., 2019. Novel approach to improve crumb rubber concrete strength using thermal treatment. *Construct. Build. Mater.* 229, 116901.
- Abhishek, H., Prashant, S., Kamath, M.V., Kumar, M., 2022. Fresh mechanical and durability properties of alkali-activated fly ash-slag concrete: a review. *Innovative Infrastructure Solutions* 7, 1–14.
- Alqahtani, F.K., Zafar, I., 2021. Plastic-based sustainable synthetic aggregate in Green Lightweight concrete—A review. *Construct. Build. Mater.* 292, 123321.
- Amran, M., Murali, G., Khalid, N.H.A., Fediuk, R., Ozbakkaloglu, T., Lee, Y.H., Haruna, S., Lee, Y.Y., 2021. Slag uses in making an ecofriendly and sustainable concrete: a review. *Construct. Build. Mater.* 272, 121942.
- Andrade, T.S., Vakros, J., Mantzavinos, D., Lianos, P., 2020. Biochar obtained by carbonization of spent coffee grounds and its application in the construction of an energy storage device. *Chemical Engineering Journal Advances* 4, 100061.
- Arulrajah, A., Kua, T.-A., Phetchuay, C., Horpibulsuk, S., Mahghoolpilehrood, F., Disfani, M.M., 2016. Spent coffee grounds—fly ash geopolymer used as an embankment structural fill material. *J. Mater. Civ. Eng.* 28 (5), 04015197.
- Arulrajah, A., Kua, T.-A., Suksiripattanapong, C., Horpibulsuk, S., Shen, J.S., 2017. Compressive strength and microstructural properties of spent coffee grounds-bagasse ash based geopolymers with slag supplements. *J. Clean. Prod.* 162, 1491–1501.
- Cao, D., Malakooti, S., Kulkarni, V.N., Ren, Y., Liu, Y., Nie, X., Qian, D., Griffith, D.T., Lu, H., 2022. The effect of resin uptake on the flexural properties of compression molded sandwich composites. *Wind Energy* 25 (1), 71–93.
- Cao, D., Malakooti, S., Kulkarni, V.N., Ren, Y., Lu, H., 2021. Nanoindentation measurement of core-skin interphase viscoelastic properties in a sandwich glass composite. *Mech. Time-Dependent Mater.* 25, 353–363.
- Chen, L., Zhang, Y., Labianca, C., Wang, L., Ruan, S., Poon, C.S., Ok, Y.S., 2022. Carbon-negative cement-bonded biochar particleboards. *Biochar* 4 (1), 1–9.
- Cuthbertson, D., Berardi, U., Briens, C., Berruti, F., 2019. Biochar from residual biomass as a concrete filler for improved thermal and acoustic properties. *Biomass Bioenergy* 120, 77–83.
- Dixit, A., Gupta, S., Dai Pang, S., Kua, H.W., 2019. Waste Valorisation using biochar for cement replacement and internal curing in ultra-high performance concrete. *J. Clean. Prod.* 238, 117876.
- El-Hassan, H., Shehab, E., Al-Sallamin, A., 2021. Effect of curing regime on the performance and microstructure characteristics of alkali-activated slag-fly ash blended concrete. *Journal of Sustainable Cement-Based Materials* 1–29.
- Eliche-Quesada, D., Martínez-García, C., Martínez-Cartas, M., Cotes-Palomino, M., Pérez-Villarejo, L., Cruz-Pérez, N., Corpas-Iglesias, F., 2011. The use of different forms of waste in the manufacture of ceramic bricks. *Appl. Clay Sci.* 52 (3), 270–276.
- Gencil, O., Karadag, O., Oren, O.H., Bilir, T., 2021. Steel slag and its applications in cement and concrete technology: a review. *Construct. Build. Mater.* 283, 122783.
- Gill, P., Roychand, R., Saberian, M., Li, J., 2023. Effects of various additives on the crumb rubber integrated geopolymer concrete. *Cleaner Materials*, 100181.
- Gravina, R.J., Xie, T., Roychand, R., Zhuge, Y., Ma, X., Mills, J.E., Youssif, O., 2021. Bond Behaviour between Crumb Rubberized Concrete and Deformed Steel Bars, Structures. Elsevier, pp. 2115–2133.
- Guo, P., Meng, W., Nassif, H., Gou, H., Bao, Y., 2020. New perspectives on recycling waste glass in manufacturing concrete for sustainable civil infrastructure. *Construct. Build. Mater.* 257, 119579.
- Gupta, S., Kua, H.W., 2017. Factors determining the potential of biochar as a carbon capturing and sequestering construction material: critical review. *J. Mater. Civ. Eng.* 29 (9), 04017086.
- Gupta, S., Kua, H.W., Dai Pang, S., 2020. Effect of biochar on mechanical and permeability properties of concrete exposed to elevated temperature. *Construct. Build. Mater.* 234, 117338.
- Gupta, S., Kua, H.W., Koh, H.J., 2018. Application of biochar from food and wood waste as green admixture for cement mortar. *Sci. Total Environ.* 619, 419–435.
- Gupta, S., Muthukrishnan, S., Kua, H.W., 2021. Comparing influence of inert biochar and silica rich biochar on cement mortar—Hydration kinetics and durability under chloride and sulfate environment. *Construct. Build. Mater.* 268, 121142.
- Gupta, S., Tulliani, J.-M., Kua, H.W., 2022. Carbonaceous admixtures in cementitious building materials: effect of particle size blending on rheology, packing, early age properties and processing energy demand. *Sci. Total Environ.* 807, 150884.
- Hu, Q., Jung, J., Chen, D., Leong, K., Song, S., Li, F., Mohan, B.C., Yao, Z., Prabhakar, A. K., Lin, X.H., 2021. Biochar industry to circular economy. *Sci. Total Environ.* 757, 143820.
- Islam, M.M.U., Li, J., Roychand, R., Saberian, M., 2023. Investigation of durability properties for structural lightweight concrete with discarded vehicle tire rubbers: a study for the complete replacement of conventional coarse aggregates. *Construct. Build. Mater.* 369, 130634.
- Islam, M.M.U., Li, J., Roychand, R., Saberian, M., Chen, F., 2022a. A comprehensive review on the application of renewable waste tire rubbers and fibers in sustainable concrete. *J. Clean. Prod.*, 133998.
- Islam, M.M.U., Li, J., Wu, Y.-F., Roychand, R., Saberian, M., 2022b. Design and strength optimization method for the production of structural lightweight concrete: an experimental investigation for the complete replacement of conventional coarse aggregates by waste rubber particles. *Resour. Conserv. Recycl.* 184, 106390.
- Jalkh, R., El-Rassy, H., Chehab, G.R., Abiad, M.G., 2018. Assessment of the physico-chemical properties of waste cooking oil and spent coffee grounds oil for potential use as asphalt binder rejuvenators. *Waste and Biomass Valorization* 9 (11), 2125–2132.
- Kilmartin-Lynch, S., Roychand, R., Saberian, M., Li, J., Chen, F., 2023. Utilisation of COVID-19 Waste PPE in the Applications of Structural Concrete, International RILEM Conference on Synergising Expertise towards Sustainability and Robustness of CBMs and Concrete Structures. Springer, pp. 521–527.
- Kilmartin-Lynch, S., Roychand, R., Saberian, M., Li, J., Zhang, G., 2021a. Application of COVID-19 Single-Use Shredded Nitrile Gloves in Structural Concrete: Case Study from Australia. *Science of The Total Environment*, 151423.
- Kilmartin-Lynch, S., Saberian, M., Li, J., Roychand, R., Zhang, G., 2021b. Preliminary evaluation of the feasibility of using polypropylene fibres from COVID-19 single-use face masks to improve the mechanical properties of concrete. *J. Clean. Prod.* 296, 126460.
- Kilmartin-Lynch, S., Roychand, R., Saberian, M., Li, J., Zhang, G., Setunge, S., 2022. A sustainable approach on the utilisation of COVID-19 plastic based isolation gowns in structural concrete. *Case Stud. Constr. Mater.* 17, e01408.
- Li, X., Ling, T.-C., Mo, K.H., 2020. Functions and impacts of plastic/rubber wastes as eco-friendly aggregate in concrete—A review. *Construct. Build. Mater.* 240, 117869.
- Liu, J., Liu, G., Zhang, W., Li, Z., Xing, F., Tang, L., 2022. Application potential analysis of biochar as a carbon capture material in cementitious composites: a review. *Construct. Build. Mater.* 350, 128715.
- Liu, S.-H., Huang, Y.-Y., 2018. Valorization of coffee grounds to biochar-derived adsorbents for CO<sub>2</sub> adsorption. *J. Clean. Prod.* 175, 354–360.
- Maghfouri, M., Alimohammadi, V., Gupta, R., Saberian, M., Azarsa, P., Hashemi, M., Asadi, I., Roychand, R., 2022. Drying shrinkage properties of expanded polystyrene (EPS) lightweight aggregate concrete: a review. *Case Stud. Constr. Mater.*, e00919.
- Melikoglu, M., Lin, C.S.K., Webb, C., 2013. Analysing global food waste problem: pinpointing the facts and estimating the energy content. *Cent. Eur. J. Eng.* 3 (2), 157–164.
- Mofijur, M., Kusumo, F., Fattah, I.R., Mahmudil, H., Rasul, M., Shamsuddin, A., Mahlia, T., 2020. Resource recovery from waste coffee grounds using ultrasonic-assisted technology for bioenergy production. *Energies* 13 (7), 1770.
- Mohamed, G., Djamil, B., 2018. Properties of Dune Sand Concrete Containing Coffee Waste, MATEC Web of Conferences. EDP Sciences, 01039.

- Muñoz Velasco, P., Mendivil, M., Morales, M., Muñoz, L., 2016. Eco-fired clay bricks made by adding spent coffee grounds: a sustainable way to improve buildings insulation. *Mater. Struct.* 49 (1), 641–650.
- Na, S., Lee, S., Youn, S., 2021. Experiment on activated carbon manufactured from waste coffee grounds on the compressive strength of cement mortars. *Symmetry* 13 (4), 619.
- Nodehi, M., Mohamad Taghvaei, V., 2022. Sustainable concrete for circular economy: a review on use of waste glass. *Glass Structures & Engineering* 7 (1), 3–22.
- Oliveira, L.S., Oliveira, D.S., Bezerra, B.S., Pereira, B.S., Battistelle, R.A.G., 2017. Environmental analysis of organic waste treatment focusing on composting scenarios. *J. Clean. Prod.* 155, 229–237.
- Perera, S.T.A.M., Saberian, M., Zhu, J., Roychand, R., Li, J., 2022. Effect of crushed glass on the mechanical and microstructural behavior of highly expansive clay subgrade. *Case Stud. Constr. Mater.* 17, e01244.
- Perera, S.T.A.M., Saberian, M., Zhu, J., Roychand, R., Li, J., Ren, G., Yamchelou, M.T., 2023. Improvement of low plasticity clay with crushed glass: a mechanical and microstructural study. *Int. J. Pavement Res. Technol.* 1–21.
- Roychand, R., 2017. Performance of Micro and Nano Engineered High Volume Fly Ash Cement Composite. RMIT University.
- Roychand, R., De Silva, S., Law, D., Setunge, S., 2016a. High volume fly ash cement composite modified with nano silica, hydrated lime and set accelerator. *Mater. Struct.* 49 (5), 1997–2008.
- Roychand, R., De Silva, S., Law, D., Setunge, S., 2016b. Micro and nano engineered high volume ultrafine fly ash cement composite with and without additives. *International Journal of Concrete Structures and Materials* 10 (1), 113–124.
- Roychand, R., De Silva, S., Setunge, S., 2018. Nanosilica modified high-volume fly ash and slag cement composite: environmentally friendly alternative to OPC. *J. Mater. Civ. Eng.* 30 (4), 04018043.
- Roychand, R., Gravina, R.J., Zhuge, Y., Ma, X., Mills, J.E., Youssf, O., 2021a. Practical rubber pre-treatment approach for concrete use—an experimental study. *Journal of Composites Science* 5 (6), 143.
- Roychand, R., Gravina, R.J., Zhuge, Y., Ma, X., Youssf, O., Mills, J.E., 2020a. A comprehensive review on the mechanical properties of waste tire rubber concrete. *Construct. Build. Mater.* 237, 117651.
- Roychand, R., Li, J., De Silva, S., Saberian, M., Law, D., Pramanik, B.K., 2021b. Development of zero cement composite for the protection of concrete sewage pipes from corrosion and fatbergs. *Resour. Conserv. Recycl.* 164, 105166.
- Roychand, R., Li, J., Kilmartin-Lynch, S., Saberian, M., Zhu, J., Youssf, O., Ngo, T., 2023a. Carbon sequestration from waste and carbon dioxide mineralisation in concrete—A stronger, sustainable and eco-friendly solution to support circular economy. *Construct. Build. Mater.* 379, 131221.
- Roychand, R., Li, J., Kilmartin-Lynch, S., Saberian, M., Zhu, J., Youssf, O., Ngo, T., 2023b. Carbon sequestration from waste and carbon dioxide mineralisation in concrete – a stronger, sustainable and eco-friendly solution to support circular economy. *Construct. Build. Mater.* 379, 131221.
- Roychand, R., Patel, S., Halder, P., Kundu, S., Hampton, J., Bergmann, D., Surapaneni, A., Shah, K., Pramanik, B.K., 2021c. Recycling biosolids as cement composites in raw, pyrolyzed and ashed forms: a waste utilisation approach to support circular economy. *J. Build. Eng.* 38, 102199.
- Roychand, R., Pramanik, B.K., Zhang, G., Setunge, S., 2020b. Recycling steel slag from municipal wastewater treatment plants into concrete applications—A step towards circular economy. *Resour. Conserv. Recycl.* 152, 104533.
- Saberian, M., Li, J., Perera, S.T.A.M., Ren, G., Roychand, R., Tokhi, H., 2020. An experimental study on the shear behaviour of recycled concrete aggregate incorporating recycled tyre waste. *Construct. Build. Mater.* 264, 120266.
- Saberian, M., Li, J., Donnoli, A., Bondarenko, E., Oliva, P., Gill, B., Lockrey, S., Siddique, R., 2021a. Recycling of spent coffee grounds in construction materials: a review. *J. Clean. Prod.* 289, 125837.
- Saberian, M., Li, J., Perera, S.T.A.M., Zhou, A., Roychand, R., Ren, G., 2021b. Large-scale direct shear testing of waste crushed rock reinforced with waste rubber as pavement base/subbase materials. *Transport. Geotech.* 28, 100546.
- Santos, C., Goufo, P., Fonseca, J., Pereira, J.L., Ferreira, L., Coutinho, J., Trindade, H., 2018. Effect of lignocellulosic and phenolic compounds on ammonia, nitric oxide and greenhouse gas emissions during composting. *J. Clean. Prod.* 171, 548–556.
- Sena da Fonseca, B., Vilão, A., Galhano, C., Simão, J., 2014. Reusing coffee waste in manufacture of ceramics for construction. *Adv. Appl. Ceram.* 113 (3), 159–166.
- Suarez-Riera, D., Restuccia, L., Ferro, G.A., 2020. The use of Biochar to reduce the carbon footprint of cement-based materials. *Procedia Struct. Integr.* 26, 199–210.
- Tan, K.-H., Wang, T.-Y., Zhou, Z.-H., Qin, Y.-H., 2021. Biochar as a partial cement replacement material for developing sustainable concrete: an overview. *J. Mater. Civ. Eng.* 33 (12), 03121001.
- Wang, X., Xu, T., de Andrade, M.J., Rampalli, I., Cao, D., Haque, M., Roy, S., Baughman, R.H., Lu, H., 2021. The interfacial shear strength of carbon nanotube sheet modified carbon fiber composites. *Challenges in Mechanics of Time Dependent Materials*. In: *Proceedings of the 2020 Annual Conference on Experimental and Applied Mechanics*, 2. Springer, pp. 25–32.
- Youssf, O., Elchalakani, M., Hassanli, R., Roychand, R., Zhuge, Y., Gravina, R.J., Mills, J. E., 2022. Mechanical performance and durability of geopolymer lightweight rubber concrete. *J. Build. Eng.* 45, 103608.
- Youssf, O., Hassanli, R., Mills, J.E., Skinner, W., Ma, X., Zhuge, Y., Roychand, R., Gravina, R., 2019. Influence of mixing procedures, rubber treatment, and fibre additives on rubcrete performance. *Journal of Composites Science* 3 (2), 41.
- Youssf, O., Mills, J.E., Benn, T., Zhuge, Y., Ma, X., Roychand, R., Gravina, R., 2020. Development of crumb rubber concrete for practical application in the residential construction sector—design and processing. *Construct. Build. Mater.* 260, 119813.
- Zhang, X., Zhang, Y., Ngo, H.H., Guo, W., Wen, H., Zhang, D., Li, C., Qi, L., 2020. Characterization and sulfonamide antibiotics adsorption capacity of spent coffee grounds based biochar and hydrochar. *Sci. Total Environ.* 716, 137015.
- Zhang, Y., He, M., Wang, L., Yan, J., Ma, B., Zhu, X., Ok, Y.S., Mechtcherine, V., Tsang, D. C., 2022a. Biochar as construction materials for achieving carbon neutrality. *Biochar* 4 (1), 1–25.
- Zhang, Y., He, M., Wang, L., Yan, J., Ma, B., Zhu, X., Ok, Y.S., Mechtcherine, V., Tsang, D. C., 2022b. Biochar as construction materials for achieving carbon neutrality. *Biochar* 4 (1), 59.
- Zhu, J., Saberian, M., Perera, S.T.A.M., Roychand, R., Li, J., Wang, G., 2022. Reusing COVID-19 disposable nitrile gloves to improve the mechanical properties of expansive clay subgrade: an innovative medical waste solution. *J. Clean. Prod.* 375, 134086.